CONDENSED MATTER

Impedance of Aqueous Solutions of KCl at the Ultra-low Frequency Range: Use of Cole-Cole Impedance Element to Account for the Frequency Dispersion Peak at 20 mHz

José A. Giacometti[1] · Neri Alves[2] · Márcia Y. Teruya[2]

Abstract This paper reports on the analysis of dispersion in the imaginary part of impedance often observed at low frequencies in a variety of systems. The experimental data were obtained with an electrolytic cell containing KCl aqueous solution in the frequency range from 0.1 mHz to 10 MHz, where the use of ultra-low frequencies helps clarify the analysis of the imaginary impedance dispersion. It is shown that the low frequency dispersion described in the literature is the tail of a relaxation peak located at $f \cong 20$ mHz. This ultra-low frequency dispersion peak is analyzed with a Cole-Cole impedance element, being associated with the electric double layer at the metal-electrolyte interface. Quantitative information can be extracted for the double layer, including its thickness (~1 nm) and electrical resistivity (~50 GΩm).

Keywords Electric double layer · Metal-electrolyte interface · Electrolytic solution · Impedance measurements · Ultra-low frequency

1 Introduction

Many studies have been performed using broadband immittance measurements in a cell containing a metal-electrolyte solution interface [1, 2], including the case of a parallel plate capacitor containing a water-KCl solution [3]. For KCl, the data above 10 kHz are explained by the bulk solution properties, and an increase was observed in both the real and imaginary parts of impedance from 10 mHz to 10 kHz. This increase is attributed to polarization at the metal-aqueous solution interface, the so-called electrical double layer. In terms of modeling, the immittance data for a KCl cell have been analyzed with the Poisson-Nernst-Planck (PNP) model, the PNP anomalous model and assuming an ionic adsorption/ desorption process at the surfaces or considering ohmic or blocking electrodes [4–9].

Alternatively, the results of immittance have been treated using equivalent circuits containing, for example, a constant phase element (CPE) [10–12]. This allows for determining the capacitance and resistance of the double layer, in addition to providing information on effects from surface roughness, electrode porosity, and geometry. Even though experimental data have been available for many years, sophisticated models and the applicability of phenomenological circuit models to fit the data are still under debate. Only recently, Lenzi et al. [13] show an analytical connection between the PNP model and the phenomenological interpretation using CPEs in equivalent circuits.

In this paper, measurements of electrical impedance of KCl aqueous solutions were extended to ultra-low frequencies, 0.1 mHz < f < 10 mHz. The aim is to analyze a broad peak at 20 mHz in the imaginary part of the impedance, which is in contrast to results from the literature [3, 14, 15]. This ultra-low frequency peak is fitted with a Cole-Cole impedance element, from which quantitative, consistent information about the double layer can be extracted, including double layer thickness, capacitance, and resistivity.

✉ José A. Giacometti
giacometti@ifsc.usp.br

1 Instituto de Física de São Carlos, USP, 13566-590 São Carlos, SP, Brazil

2 Faculdade de Ciências e Tecnologia, UNESP, 19060-900 Presidente Prudente, SP, Brazil

2 Experimental Data

The parallel plate capacitor consisted of polished gold-plated brass electrodes 2 cm in diameter and 1.3 mm apart, mounted inside a Plexiglass cell hermetically closed after filling with KCl solution. The cell was held inside an aluminum Faraday cage to minimize electric interference during impedance measurements. The distance of 1.3 mm between electrodes was not varied in the measurements. Before each measurement, the Au electrodes and the container were cleaned with Milli-Q water and dried by flushing nitrogen gas. All measurements were performed at 22±0.5 °C using a temperature-controlled bath. The KCl solutions with concentrations of 0.3, 0.45, and 0.6 mM were prepared using ultra-pure Milli-Q water (18.2 MΩcm). KCl was purchased from Aldrich and used as received.

Electric impedance measurements were carried out using a 1260A Solartron analyzer and with a 1296A dielectric interface in the frequency range 0.1 mHz$<f<$10 MHz applying an *ac* voltage of 50 mV. In order to optimize data collection, the impedance measurements were performed using different experimental conditions: (a) at 1 MHz$<f<$10 MHz, an impedance matcher was employed with the 1260A analyzer [16], and (b) for 0.1 mHz$<f<$1 MHz the 1260A analyzer and the 1296A dielectric interface were used. In the range 100 mHz$<f<$1 MHz, the analyzer was set to measure the signal response during several periods of the *ac* voltage (integration time of the 1260A analyzer) to guarantee an accuracy with dispersion smaller than 1 % and high rejection of all harmonic frequencies. At the ultra-low frequency range, 0.1 mHz$<f<$100 mHz, measurements were time consuming and, therefore, the signal was integrated over one period of the *ac* voltage only. Although measurements over just one period provides only a reasonable rejection of all harmonic frequencies, it will be shown that reliable impedance could still be obtained. The real and imaginary impedance data were fitted simultaneously using the ZView software [17].

3 Results and Discussion

Figure 1 shows the frequency dependence for the real and imaginary impedances in the frequency range 0.1 mHz$<f<$10 MHz for various concentrations of KCl aqueous solutions. The impedance measurements with the KCl cell did not depend on the applied *ac* voltage up to 100 mV; larger *ac* amplitudes were not attempted. Worth to mention is that the real and imaginary parts of impedance are consistent since they satisfy very well the Kramer-Kronig [18] relation except at frequencies above few megahertz. Furthermore, our data is in good agreement with the ones published elsewhere [14, 15] considering the area, distance between electrodes, and the KCl concentration.
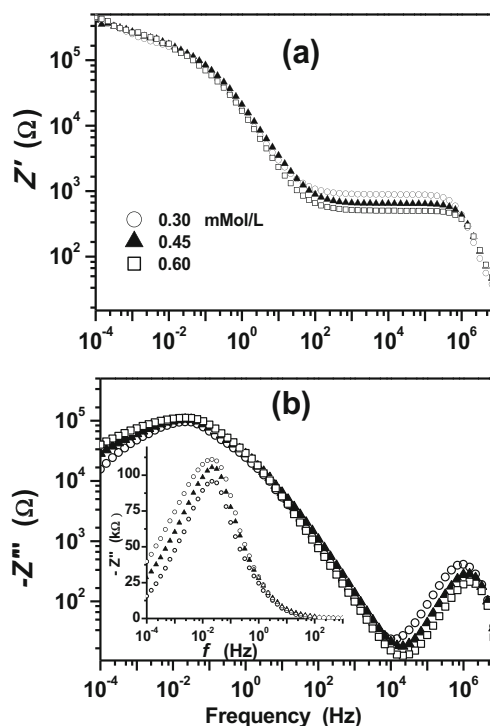

Fig. 1 **a** Real part and **b** imaginary part of the complex impedance of the KCl solution for different values of the KCl concentration. The inset shows the ultra-low frequency peak (linear scale) separately

The real part of the impedance decreased with frequency, featuring a plateau for 100 Hz$<f<$1 MHz. The plateau and the decrease of the real part above ~1 kHz are due to ionic conduction of K^+ and Cl^- ions in the solution bulk [3]. The plateau height, a measure of the cell electric resistance, decreased with KCl concentration since electric conduction across the bulk is proportional to the ionic concentration, as it is confirmed from data in Fig. 1a. The imaginary part of the electric impedance displays two peaks; the broad one at $f \cong 20$ mHz had never been reported to the best of our knowledge. We assume that the imaginary impedance data for KCl cell reported in the literature for $f>10$ mHz is the tail of the peak at $f \cong 20$ mHz shown here. The peak for $f \cong 1$ MHz is known to arise from the conduction of K^+ and Cl^- ions across the solution bulk [3].

Data in Fig. 1 were further analyzed by calculating the real and imaginary dielectric constants as shown in Fig. 2. The real part of the dielectric constant increased from 80 to about 10^8 as the frequency decreased, being almost independent of the KCl concentration, thus indicating a strong capacitive effect. This behavior is typical of an interfacial polarization, and therefore consistent with the hypothesis of an electric double layer at the metal-electrolyte interface. The imaginary part of the dielectric constant also increased at the low frequency with a shoulder at ~1 kHz. Here, we will assume that the aqueous solution is a dispersive, conductive system, and in the frequency range used, dipolar and vibratory effects lead to a
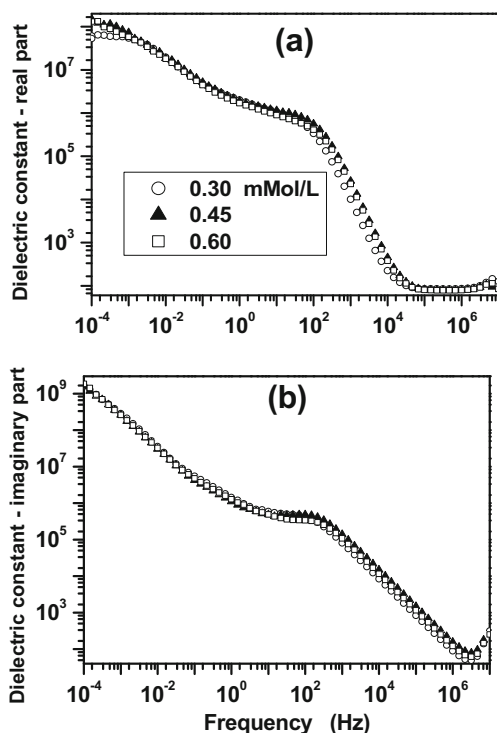
Fig. 2 Dependence of dielectric constant on frequency. **a** Real part and **b** imaginary part

frequency-independent bulk dielectric constant [19, 20]. This hypothesis is supported by the complex dielectric data in Fig. 2 displaying a steady increase for imaginary dielectric constant in the frequency range from 0.1 mHz to 10 MHz.

As mentioned in Section 1, so far, the steady increase in impedance at low frequencies has been explained using equivalent circuits containing a constant phase element [10–12] and PNP models [4, 5, 7–9]. None of these works considered an ultra-low frequency peak at $f\cong20$ mHz in the imaginary part of the impedance. Next, we will show that a Cole-Cole impedance element satisfactorily describes the immittance data at ultra-low frequencies and gives adequate values for thickness and electric resistance of the electric double layer although the circuit element is not a physical model.

The impedance curves in Fig. 1 were analyzed using the equivalent electric circuit depicted in Fig. 3. The parallel $R_B C_B$ circuit represents the high frequency conductive response of ions in the solution bulk, and the Cole-Cole impedance element is used to represent the ultra-low frequency response of the KCl cell. The Cole-Cole impedance element provides a
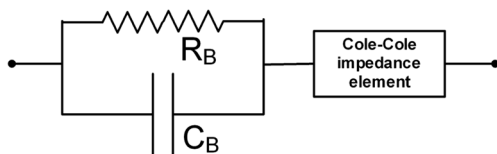

Fig. 3 Equivalent circuit to represent a capacitor filled with the KCl solution

wide peak at ultra-low frequency necessary for the fitting. Its expression is given by

$$Z_C^* = \frac{R_C}{1 + (j\omega C_C R_C)^\beta} \qquad (1)$$

where R_c has the physical dimension of ohms, $j = \sqrt{-1}$, and $\omega=2\pi f$; C_C is an electric capacitance and β is the Cole-Cole constant ($0<\beta<1$).

The curves that fit the experimental data for a KCl concentration of 0.3 mM is shown in Fig. 4, with the corresponding parameters of the equivalent circuit being given in Table 1. It is worth mentioning that our fitting covers a broad frequency range that varies over 11 orders of magnitude, 0.1 mHz<f< 10 MHz. Data fitting for the concentrations of 0.45 and 0.6 mM leads to results similar to those in Fig. 4 and were therefore omitted. Table 1 shows R_B decreasing proportionally with KCl concentration as expected, while C_B, R_C, C_C, and β are nearly independent of the KCl concentration. The value of C_C is the main parameter to determine the position of the ultra-low frequency peak. The accuracy with which C_C can be determined from the fittings is ca. 10 %, while for C_B, R_C, and β, the accuracy is within a few percent. The insets in Fig. 1b show that the ultra-low frequency peak is asymmetric, being wider on the low frequency side ($f<10^{-2}$ Hz) in a region where fitting is poorer. This behavior cannot be exactly accounted with the Cole-Cole impedance element since it provides a symmetric peak in contrast to our data. Attempts to fit
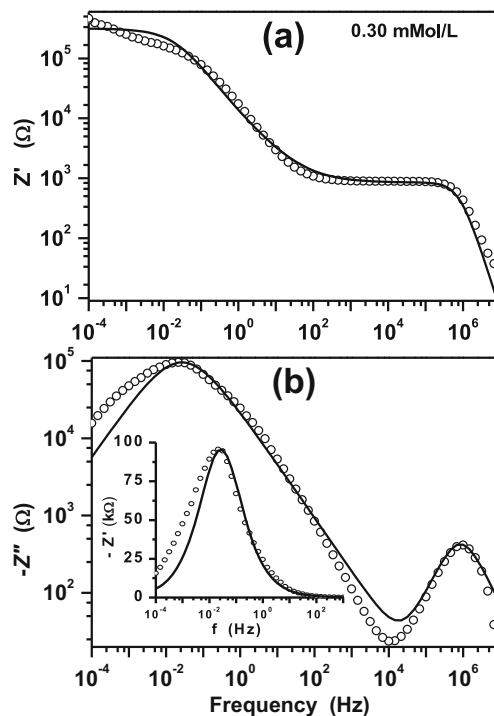

Fig. 4 Experimental data for the complex impedance (*circles*) and the fitting curves (*solid lines*) employing Eq. (1). The inset on the right figure shows separately the ultra-low frequency peak (*linear scale*)

Table 1 Values of the circuit parameters obtained from fitting the experimental curves. R_B, C_B, R_C, C_C, and β are the parameters given in Eq. (1)

Concentration mM	R_B (Ω)	C_B (pF)	R_C (kΩ)	C_C (μF)	β
0.30	788	194	317	19.4	0.69
0.45	567	179	302	13.7	0.70
0.60	437	172	328	14.4	0.73

the data with a Cole-Davidson impedance element (where the denominator of Eq. (1) is replaced by $(1+j\omega\tau)^{\alpha}$) systematically gave a poorer fitting than the Cole-Cole circuit element, since the Cole-Davidson expression predicts a wider peak at its right side. Also, the peak at ~1 MHz is not so well fitted for $f>5$ MHz because the Cole-Cole peak has a tail at high frequencies, in addition to the lack of accuracy in the measurements with the 1260A analyzer. The effects mentioned above lead to a rather low precision for the fittings, i.e., χ^2 is approximately 0.1.

The impedance spectra for 100 Hz$<f<10$ MHz are determined by the movement of K$^+$ and Cl$^-$ ions through the solution bulk [3], represented by the $R_B C_B$ parallel circuit in Fig. 3. Thus, R_B and C_B obtained from the fitting allow the bulk properties of the KCl solution to be determined. For example, the ion mobility, μ, can be determined using $R_B=L/A\sigma=L/2Aqn\mu$, where n is the ionic concentration, $A=3.14$ cm^2 is the electrode area, L is the electrode separation, and σ is the electrical conductivity (K$^+$ and Cl$^-$ ions are assumed to have the same mobility). Table 2 shows that the mobility is almost independent of concentration. Its mean value $(8.1\pm0.8)\times10^{-8}$ cm^2/Vs calculated over the three KCl concentrations agrees with the known mobility for K$^+$ (7.6×10^{-8} cm^2/Vs) and Cl$^-$ (7.9×10^{-8} cm^2/Vs) ions in water at 22 °C. The $R_B C_B$ parallel circuit is frequently used to account for the high frequency response of electrolytic cells, which is also in agreement with the theoretical model by Becchi et al. [3].

As shown in Fig. 4, the impedance spectra in the ultra-low frequency range can be fitted reasonably using the Cole-Cole impedance element in Eq. (1). Although there is a deviation on the left side of the peak for the reason mentioned before, we propose a phenomenological description of the electric double layer on the electrode interface. For instance, we assume that R_C and C_C are a measure of the electric resistance and the capacitance of the electric double layer. One should recall that two electric double layers exist in the cell, one at each electrode; thus, the capacitance of one double layer is $C_D=2C_C$ and its resistance is $R_D=R_C/2$.

Table 2 shows that R_D and C_D are both practically independent of the KCl concentration. The capacitance of the double layer C_D is ~31 μF, i.e., ~10 μF/cm^2, in agreement with values published elsewhere [21]. From the electric double layer capacitance, we determined the double-layer thickness $L_D\cong1$ nm, independent of the KCl concentration (see Table 2), assuming a dielectric constant of 10 for water trapped between the double-charged layers [6]. This thickness corresponds to two layers of water molecules, being consistent with the Helmholtz model for the electric double layer. Since $L_D\cong1$ nm and $R_D\cong160$ kΩ, the electric resistivity of the double layer is estimated to be ~5×10^{10} Ωm, which is very high as expected.

The success of the Cole-Cole phenomenological interpretation is not surprising in view of the many efforts [22–24] to account for the increase in impedance of aqueous electrolytic solutions at low frequencies using a CPE impedance element. As shown by Lenzi et al. [13], there are analytical connections between the Poisson-Nernst-Planck model and equivalent circuits containing constant phase elements. In our case, for $f>$~0.03 Hz, the modulus of $(j\omega C_C R_C)^{\beta}$ becomes larger than one, and for the frequency range above this limit, the Cole-Cole Eq. (1) reduces to its imaginary part ~$\frac{R_C}{(j\omega C_C R_C)}{}^{\beta}$, that is, the Cole-Cole circuit becomes a CPE element circuit. As Table 1 shows a value of $\beta\cong0.7$ is in agreement with the slope found in the imaginary impedance (in the range of frequency from kHz to 0.01 Hz) for electrodes of platinum and gold [15].

We also made a few experiments employing mixtures of ethanol and Milli-Q water (results not shown here). With ethanol-water mixtures in the cell, a similar behavior to the KCl solution was found. The high frequency peak appeared at $f\cong100$ kHz, while the ultra-low frequency peak was observed at $f\cong2$ mHz (lower than for KCl), independently of the water content. Such results show that the ultra-low frequency peak depends on the liquid also confirming that the ultra-low frequency peak is not an experimental artifact.

Table 2 Values for mobility, μ, double layer capacitance, C_D, double-layer resistance, R_D, obtained from the fitting. L_D is the double-layer thickness

Concentration of KCl (mM)	Concentration of KCl (10^{23} m^{-3})	μ 10^{-8} (m^2/Vs)	R_D (kΩ)	C_D (μF)	L_D (nm)
0.30	1.8	8.5	158	38	0.7
0.45	2.7	7.9	151	27	1.0
0.60	3.6	8.0	164	29	1.0

4 Conclusions

We have investigated the ultra-low frequency impedance response of a cell filled with ions of KCl dissolved in water. The cell volume is responsible for the high frequency spectra of the impedance, represented here by a parallel RC circuit. This is

plausible since it is equivalent to a Debye conductive relaxation process [25] or to the physical model given by Becchi et al. [3]. We found that the mobility of ions, circa of 8×10^{-8} m^2/Vs, is practically independent of the KCl concentration and in good agreement with known values for K$^+$ and Cl$^-$.

The broad peak at the ultra-low frequency around 20 mHz in the imaginary part of the impedance is attributed to the formation of the Helmholtz electric double layer at the metal interface. In spite of the simplicity of the Cole-Cole circuit, it is possible to establish a simple relationship between the circuit model and physical parameters. The thickness $L_D \cong 1$ nm for the double layer is in good agreement with the Helmholtz double layer and values measured experimentally [26]. The Debye length $\left(\frac{\varepsilon k T}{2 n q}\right)^{1/2}$ (symbols have the usual meaning) found from our data decreases from 6.5 to 4.5 nm when the concentration varied from 0.3 to 0.6 mM indicating that the outside Helmholtz plane of the double layer is within the Debye layer. The Cole-Cole constant $\beta \cong 0.7$ indicated a dispersive electric conduction, with the distribution of relaxation processes being ascribed to a distribution of double layer capacitances which depend on parameters such as the surface roughness of the electrodes [13].

Further insights into the ultra-low frequency peak will require detailed measurements where systematic changes are used for cell geometry; area of electrodes, their roughness, and different electrolytes are employed. For example, we suggest that the ultra-low frequency peak can be shifted to higher frequencies by decreasing the double layer capacitance C_D (e.g., decreasing the electrode area). This is important from a practical point of view to save time in the measurements and get more details of the left side of the peak.

Also relevant is to identify physical models that can explain the impedance data, for instance by using Poisson-Nernst-Planck continuum equations of charge motion in liquids of an electrochemical cell, as extensively discussed in literature [14, 27, 28]. One candidate to explain the low frequency peak is to consider ohmic electrodes [14] that show two alike peaks in the imaginary impedance spectra. Other possibilities for physical interpretation are the model considering diffusion proposed by Macdonald [27] and the model by Lenzi et al. [29] based on fractional diffusion with special boundary conditions with ohmic electrodes.

With regard to equivalent circuit elements, further analysis and work are necessary to improve fitting of the data, which will probably require addition of new elements to the circuit.

References

1. J.R. Macdonald, W.B. Johnson, *Impedance Spectroscopy* (Wiley & Sons, New York, 1987)
2. F. Kremer, A. Schönhals (eds.), *Broadband Dielectric Spectroscopy* (Springer, Germany, 2003)
3. M. Becchi, C. Avendano, A. Stragazzi, G. Barbero, Impedance Spectroscopy of water solutions: the role of ions at the liquid-electrode interface. J. Chem. Phys. B **109**, 23444–23449 (2005)
4. G. Barbero, L.R. Evangelista, Adsorption phenomena of neutral particles and a kinetic equation at the interface. Phys. Rev. E **70**, 031605 (2004)
5. G. Barbero, Influence of adsorption phenomenon on the impedance spectroscopy of a cell of liquid. Phys. Rev. E **71**, 062201 (2005)
6. G. Barbero, A.M. Figueiredo Neto, F.C.M. Freire, M. Scarlerandi, Frequency dependence of the electrical impedance of electrolytic cells: the role of the ionic adsorption/desorption phenomena and the Stern layer. Phys. Lett. A **360**, 179–182 (2006)
7. G. Barbero, M. Becchi, A. Stragazzi, J. Le Digabel, A.M. Figueiredo Neto, Experimental evidence for the adsorption-desorption phenomenon of the spectroscopy impedance measurements of an electrolytic cell. J. Appl. Phys. **101**, 044102 (2007)
8. G. Derfel, G. Barbero, Numerical study of ionic contribution to susceptibility and impedance of dielectric layer. J. Mol. Liq. **150**, 43–50 (2009)
9. G. Barbero, F. Batalioto, A.M. Figueiredo Neto, Impedance spectroscopy of an electrolytic cell limited by ohmic electrodes. J. Appl. Phys. **101**, 054102 (2007)
10. D.M. Taylor, A.G. MacDonald, AC admittance of the metal-insulator-electrolyte interface. J. Phys. D. Appl. Phys. **20**, 1277–1283 (1987)
11. J.-B. Jorcim, M.E. Orazem, N. Pebere, B. Tribollet, CPE analysis by local electrochemical impedande spectroscopy. Electrochim. Acta **51**, 1473–1479 (2006)
12. W.G. Pell, A. Zolfaghari, B.E. Conway, Capacitance of the double-layer at polycrystalline Pt electrodes bearing a surface-oxide film. J. Electroanal. Chem. **532**, 13–23 (2002)
13. E.K. Lenzi, J.L. de Paula, F.R.G.B. Silva, L.R. Evangelista, A connection between anomalous Poisson-Nernst-Planck model and equivalent circuits with constant phase elements. J. Chem. Phys. C **117**, 23685–23690 (2013)
14. A.R. Duarte, F. Batalioto, G. Barbero, A.M. Figueiredo Neto, Measurement of the impedance of aqueous solutions of KCl: an analysis using an extension of Poisson-Nernst-Planck model. Appl. Phys. Lett. **105**, 022901 (2014)
15. A.R. Duarte, Ph.D. Thesis, São Paulo University, Brazil (2015)
16. As described in the 1260A Impedance Analyzer operating manual
17. Scribner and Associates, Inc., Charlottesville, VA, USA
18. R.H.M. van de Leur, A critical consideration on the interpretation of impedance plots. J. Phys. D. Appl. Phys. **24**, 1430–1435 (1991)
19. J.R. Macdonald, Comparison and evaluation of several models for fitting the frequency response of dispersive systems. J. Chem. Phys. **118**, 3258–3267 (2003)
20. J.R. Macdonald, Analysis of dielectric and conductive dispersion above T$_g$ in glass-forming molecular liquids. J. Chem. Phys. **112**, 13684–13694 (2008)
21. K.J. Woelfel, J.E. Pemberton, Determination of emersed electrochemical interface thickness by ellipsometry: aqueous electrolytes on Ag. J. Electroanal. Chem. **456**, 161–169 (1998)
22. J.B. Bates, Y.T. Chu, W.T. Stribling, Surface topography and impedance of metal-electrolytic interfaces. Phys. Rev. Lett. **60**, 627–630 (1988)
23. F. Pizzitutti, F. Bruno, Electrode and interfacial polarization in broadband dielectric spectroscopy measurements. Rev. Sci. Instrum. **72**, 2502–2504 (2001)

24. V.M.-W. Huang, V. Vivier, M.E. Orazem, N. Pébère, B. Tribollet, The apparent constant-phase-element behavior of a disk electrode with faradaic reactions—a global and local impedance analysis. J. Electrochem. Soc. **154**, C81–C88 (2007)

25. F. Batalioto, A.R. Duarte, G. Barbero, A.M. Figueiredo Neto, Dielectric dispersion of water in the frequency range from 10 mHz to 30 MHz. J. Phys. Chem. B **114**, 3467–3471 (2010)

26. K.J. Woefel, J.E. Pemberton, Determination of emersed electrochemical interface thickness by ellipsometry: aqueous electrolytes on Ag. J. Electroanal. Chem. **456**, 161–169 (1998)

27. J.R. Macdonald, Utility of continuum diffusion models for analyzing mobile-ion immittance data: electrode polarization, bulk, and generation-recombination effects. J. Phys. Condens. Matter **22**, 495101 (2010)

28. J.R. Macdonald, Utility and importance of Poisson-Nernst-Planck immittance spectroscopy fitting models. J. Chem. Phys. C **117**, 23433–23450 (2013)

29. E.K. Lenzi, M.K. Lenzi, F.R.G.B. Silva, G. Gonçalves, R. Rossato, R.S. Zola, L.R. Evangelista, A framework to investigate the immittance responses for finite length-situations: fractional diffusion equation, reaction term, and boundary conditions. J. Electroanal. Chem. **712**, 82–88 (2014)